Bled Workshops
in Physics
Vol. 13, No. 1
p. 66

Proceedings of the Mini-Workshop
Hadronic Resonances
Bled, Slovenia, July 1 - 8, 2012

Meson electro-production in the region of the Delta(1700) D33 resonance

B. Golli

Faculty of Education, University of Ljubljana, 1000 Ljubljana, Slovenia and Jožef Stefan Institute, 1000 Ljubljana, Slovenia

Abstract. We apply a coupled channel formalism incorporating quasi-bound quark-model states to calculate the D13, D33 and D15 scattering and electro-production amplitudes. The meson-baryon vertices for πN, $\pi\Delta$ (s- and d-waves), ρN, $\pi N(1440)$, $\pi N(1535)$, $\pi\Delta(1600)$ and $\sigma\Delta(1600)$ channels are determined in the Cloudy Bag Model. We use the same values for the model parameters as in the case of the P11, P33 and S11 partial waves except for the strength of the coupling of the d-wave mesons to quarks which has to be increased in order to reproduce the width of the observed D-wave resonances. The electro-production amplitudes exhibit a consistent behavior in all channels but are too weak in the resonance region.

1 Introduction

This work is a continuation of a joint project on the description of baryon resonances performed by the Coimbra group (Manuel Fiolhais and Pedro Alberto) and the Ljubljana group (Simon Širca and B. G.) [1–9]. In our previous works [5–7] we have successfully applied our method which incorporates excited baryons represented as quasi-bound quark-model states into a coupled channel formalism using the K-matrix approach [5] to calculate the scattering and the electro-production amplitudes in the P11, P33 and S11 partial waves. In the present work we extend of the approach to low lying negative parity D-wave resonances.

In the next section we give a short review of the method and in the following sections we discuss in more detail scattering and electro-production in the D13 and D33 and D15 partial waves.

2 The method

We limit ourselves to a class of chiral quark models in which mesons couple linearly to the quark core. In such cases the elements of the K matrix in the basis with good total angular momentum J and isospin T can be cast in the form [5]:

$$K^{JT}_{M'B'MB} = -\pi\mathcal{N}_{M'B'}\langle\Psi^{MB}_{JT}\|V_{M'}(k)\|\widetilde{\Psi}_{B'}\rangle\,, \qquad \mathcal{N}_{MB} = \sqrt{\frac{\omega_M E_B}{k_M W}}\,. \qquad (1)$$

Here ω_M and k_M are the energy and momentum of the incoming (outgoing) meson, $|\widetilde{\Psi}_B\rangle$ is properly normalized baryon state and E_B is its energy, W is the invariant energy of the meson-baryon system, and $|\Psi^{MB}\rangle$ is the principal value state

$$|\Psi^{MB}_{JT}\rangle = \mathcal{N}_{MB}\left\{[a^\dagger(k_M)|\widetilde{\Psi}_B\rangle]^{JT} + \sum_{\mathcal{R}} c^{MB}_{\mathcal{R}}|\Phi_{\mathcal{R}}\rangle + \sum_{M'B'}\int \frac{dk\,\chi^{M'B'MB}(k,k_M)}{\omega_k + E_{B'}(k) - W}\,[a^\dagger(k)|\widetilde{\Psi}_{B'}\rangle]^{JT}\right\}. \tag{2}$$

The first term represents the free meson (π, η, ρ, K, ...) and the baryon (N, Δ, Λ, ...) and defines the channel, the next term is the sum over *bare* tree-quark states $\Phi_{\mathcal{R}}$ involving different excitation of the quark core, the third term introduces meson clouds around different isobars, $E(k)$ is the energy of the recoiled baryon. We assume that the two pion decay proceeds either through an unstable meson (ρ-meson, σ-meson, ...) or through a baryon resonance ($\Delta(1232)$, $N^*(1440)$ ...). The meson amplitudes $\chi^{M'B'MB}(k,k_M)$ are proportional to the (half) off-shell matrix elements of the K-matrix and are determine by solving a Lippmann-Schwinger type of equation. The resulting matrix elements of the K-matrix take the form

$$K_{M'B'MB}(k,k_M) = -\sum_{\mathcal{R}}\frac{\mathcal{V}^M_{B\mathcal{R}}(k_M)\mathcal{V}^{M'}_{B'\mathcal{R}}(k)}{Z_{\mathcal{R}}(W)(W-W_{\mathcal{R}})} + K^{bkg}_{M'B'MB}(k,k_M), \tag{3}$$

where the first term represents the contribution of various resonances while $K^{bkg}_{M'B'MB}(k,k_M)$ originates in the non-resonant background processes. Here $\mathcal{V}^M_{B\mathcal{R}}$ is the dressed matrix element of the quark-meson interaction between the resonant state and the baryon state in the channel MB, and $Z_{\mathcal{R}}$ is the wave-function normalization. The physical resonant state $\mathcal{R}$ is a superposition of the dressed states built around the bare 3-quark states $\Phi_{\mathcal{R}'}$. The T matrix is finally obtained by solving the Heitler's equation

$$T_{MB\,M'B'} = K_{MB\,M'B'} + i\sum_{M''B''} T_{MB\,M''B''}K_{M''B''\,M'B'}. \tag{4}$$

Considering meson electro-production, the T matrix for $\gamma N \to MB$ satisfies

$$T_{MB\,\gamma N} = K_{MB\,\gamma N} + i\sum_{M'B'} T_{MB\,M'B'}K_{M'B'\gamma N}. \tag{5}$$

In the vicinity of a chosen resonance ($\mathcal{R}$) we write (see (3)):

$$K_{MB\,\gamma N} = -\frac{\mathcal{V}^M_{B\mathcal{R}}\mathcal{V}^\gamma_{N\mathcal{R}}}{Z_{\mathcal{R}}(W)(W-W_{\mathcal{R}})} - \sum_{\mathcal{R}'\neq\mathcal{R}}\frac{\mathcal{V}^M_{B\mathcal{R}'}\mathcal{V}^\gamma_{N\mathcal{R}'}}{Z_{\mathcal{R}'}(W)(W-W_{\mathcal{R}'})} + B^{bkg}_{MB\,\gamma N}. \tag{6}$$

We manipulate the first term:

$$\frac{\mathcal{V}^M_{B\mathcal{R}}\mathcal{V}^\gamma_{N\mathcal{R}}}{Z_{\mathcal{R}}(W)(W-W_{\mathcal{R}})} = \frac{{\mathcal{V}^M_{B\mathcal{R}}}^2}{Z_{\mathcal{R}}(W)(W-W_{\mathcal{R}})}\,\frac{\mathcal{V}^\gamma_{N\mathcal{R}}}{\mathcal{V}^M_{B\mathcal{R}}} = \left(K_{MB\,MB} - K^{bkg}_{MB\,MB}\right)\,\frac{\mathcal{V}^\gamma_{N\mathcal{R}}}{\mathcal{V}^M_{B\mathcal{R}}}$$

so that (5) takes the form

$$\begin{aligned} T_{MB\,\gamma N} &= \left(K_{MB\,MB} + i \sum_{M'B'} T_{MB\,M'B'} K_{M'B'\,MB} \right) \frac{\mathcal{V}^{\gamma}_{N\mathcal{R}}}{\mathcal{V}^{M}_{B\mathcal{R}}} \\ &\quad + K^{bkg}_{MB\,\gamma N} + i \sum_{M'B'} T_{MB\,M'B'} K^{bkg}_{M'B'\,\gamma N} \\ &= \frac{\mathcal{V}^{\gamma}_{N\mathcal{R}}}{\mathcal{V}^{M}_{B\mathcal{R}}} T_{MB\,MB} + T^{bkg}_{MB\,MB} \equiv T^{res}_{MB\,\gamma N} + T^{bkg}_{MB\,\gamma N} , \end{aligned} \tag{7}$$

which means that the T matrix for elektro-production can be split into the resonant part and the background part; the latter is the solution of the Heitler equation with the "background" K-matrix defined as

$$K^{bkg}_{MB\,\gamma N} = -K^{bkg}_{MB\,MB} \frac{\mathcal{V}^{\gamma}_{N\mathcal{R}}}{\mathcal{V}^{M}_{B\mathcal{R}}} - \sum_{\mathcal{R}' \neq \mathcal{R}} \frac{\mathcal{V}^{M}_{B\mathcal{R}'} \mathcal{V}^{\gamma}_{N\mathcal{R}'}}{Z_{\mathcal{R}'}(W)(W - W_{\mathcal{R}'})} + B^{bkg}_{MB\,\gamma N} .$$

Note that $\mathcal{V}^{\gamma}_{N\mathcal{R}}(k_\gamma)$ is proportional to the helicity amplitudes while the strong amplitude $\mathcal{V}^{M}_{B\mathcal{R}}(k_M)$ to $\sqrt{\Gamma_{MB}}$ and to ζ, the sign of the phase of the meson decay.

3 The D-wave resonances in the Cloudy Bag Model

In the quark model, the negative parity D-wave resonances are described by a single quark $l = 1$ orbital excitation. The two D13 (flavor octet, $J = \frac{3}{2}$) resonances are the superposition of the $S = \frac{1}{2}$ and $S = \frac{3}{2}$ configurations, the D33 resonance (flavour decouplet) has $S = \frac{1}{2}$, while the D15 resonance (octet, $J = \frac{5}{2}$) has $S = \frac{3}{2}$. We use the j–j coupling scheme in which the resonances take the following forms:

$$\begin{aligned} N(1520)D13 &= -\sin\vartheta_d |^4\mathbf{8}_{3/2}\rangle + \cos\vartheta_d |^2\mathbf{8}_{3/2}\rangle \\ &= c^1_S |(1s)^2 1p_{3/2}\rangle_{MS} + c^1_A |(1s)^2 1p_{3/2}\rangle_{MA} + c^1_P |(1s)^2 1p_{1/2}\rangle , \end{aligned} \tag{8}$$

$$\begin{aligned} N(1700)D13 &= \cos\vartheta_d |^4 8_{3/2}\rangle + \sin\vartheta_d |^2 8_{3/2}\rangle \\ &= c^2_S |(1s)^2 1p_{3/2}\rangle_{MS} + c^2_A |(1s)^2 1p_{3/2}\rangle_{MA} + c^2_P |(1s)^2 1p_{1/2}\rangle , \end{aligned} \tag{9}$$

$$\Delta(1700)D33 = |^2\mathbf{10}_{3/2}\rangle = \frac{\sqrt{5}}{3} |(1s)^2 1p_{3/2}\rangle - \frac{2}{3} |(1s)^2 1p_{1/2}\rangle , \tag{10}$$

$$N(1675)D15 = |^4\mathbf{8}_{5/2}\rangle = |(1s)^2 1p_{3/2}\rangle . \tag{11}$$

Here MS and MA denote the mixed symmetric and the mixed antisymmetric representation, and

$$c^1_S = \frac{2}{3} \sin\vartheta_d + \sqrt{\frac{5}{18}} \cos\vartheta_d , \quad c^1_A = -\frac{\sqrt{2}}{2} \cos\vartheta_d , \quad c^1_P = -\frac{\sqrt{5}}{3} \sin\vartheta_d + \frac{\sqrt{2}}{3} \cos\vartheta_d . \tag{12}$$

The $l = 2$ pions couple only to $j = 3/2$ quarks; the corresponding interaction in the Cloudy Bag Model takes the form

$$V^{\pi}_{2mt}(k) = \frac{1}{2f_\pi} \sqrt{\frac{\omega_{p_{3/2}} \omega_s}{(\omega_{p_{3/2}} - 2)(\omega_s - 1)}} \frac{\sqrt{2}}{2\pi} \frac{k^2}{\sqrt{\omega_k}} \frac{j_2(kR)}{kR} \sum_{i=1}^{3} \tau_t(i)\, \Sigma^{[\frac{1}{2}\frac{3}{2}]}_{2m}(i) , \tag{13}$$

where

$$\Sigma^{[\frac{1}{2}\frac{3}{2}]}_{1m} = \sum_{m_s m_j} C^{\frac{1}{2}m_s}_{\frac{3}{2}m_j 1m} |s m_s\rangle\langle p_{3/2} m_j|\,, \qquad \omega_s = 2.043\,, \quad \omega_{p_{3/2}} = 3.204\,.$$

In the case of P11, P33 and S11 waves we have used the bag radius $R = 0.83$ fm which determines the range of quark-pion interaction corresponding to the cut-off $\Lambda \sim 550$ MeV/c, and the value for $f_\pi = 76$ MeV which reproduces the experimental value of the πNN coupling constant. For the d-wave pions it turns out that the range predicted by (13) is too large while the resulting coupling strength is too weak. We have therefore modified the interaction in such a way as to correspond to $\Lambda \sim 550$ MeV/c, while the coupling strength has been increased by a factor 1.7 – 2.75 (depending on the considered resonance).

4 Scattering amplitudes

The effect of the form factor and the strength of quark-meson coupling discussed in the previous section is most clearly seen in the case of the D15 where the background effects as well as the influence of other resonances are almost negligible. Using our standard value for the cut-off parameter we have to increase the quark model coupling constant by a factor of 2.75 in order to obtain an almost perfect fit to the data in the region of the resonance.

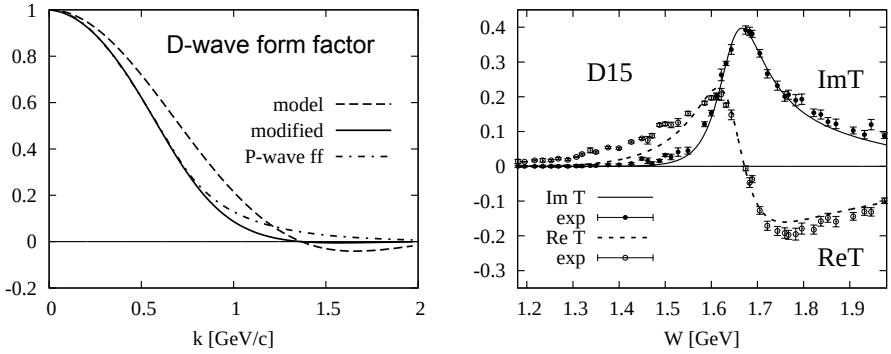

Fig. 1. The form factor for the D-wave pions (left panel), and the real and the imaginary part of the D15 scattering amplitude (right). The data points are from [10].

The data for elastic scattering in the D13 partial wave show almost no sign of the second resonance N(1700). Since the $l = 2$ pions most strongly couple to the $|(1s)^2 1p_{3/2}\rangle_{MA}$ configuration, the absence of the second resonance can be most easily explained by the vanishing of the c^2_A coefficient in (9), $c^2_A = -\sin\theta_d/\sqrt{2}$. This suggests $\theta_d = 0$. In our model the resonances are mixed through the pion interaction which changes slightly the above conclusion leading to the choice $\theta_d \approx 10^\circ$ for the optimal mixing. At this energy range the effect of the cut-off is less pronounced; the quark-model prediction for the πNR coupling constant has to be increased by a factor of 1.7, while that to the Δ decreased by a factor of one half.

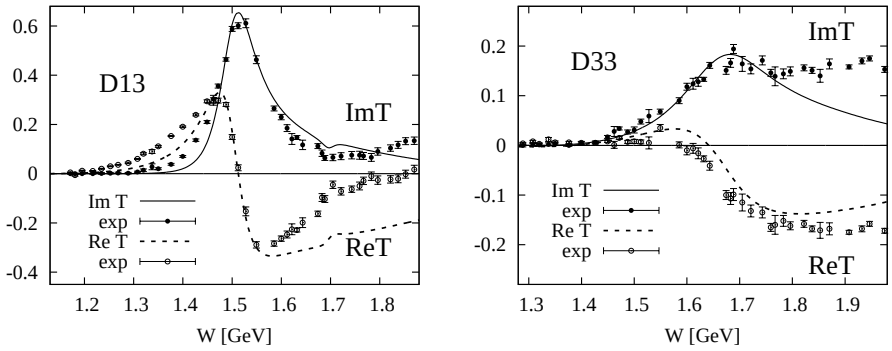

Fig. 2. The real and the imaginary part of the D13 wave scattering amplitude (left), and for the D33 wave (right). The data points are from [10].

In the vicinity of the D33 resonance the elastic amplitude is dominated by the coupling of the elastic channel to the $\pi\Delta(1232)$ channel. The d-wave pion coupling to the nucleon is increased by a factor of 2.5 with respect to the quark model value, while the model value for s-wave coupling to the $\Delta(1232)$ is not modified. Increasing the latter coupling brings the real part of the amplitude closer to the data, however the behavior of the photo-production amplitudes, presented in the next section, is deteriorated.

5 Electro-production

The electro-production amplitudes are obtained by evaluating the EM current consisting of the quark and the pion part between the nucleon ground state and the resonant state. The corresponding helicity amplitude $\mathcal{V}^{\gamma}_{N\mathcal{R}}$ in (7) reads

$$\mathcal{V}^{\gamma}_{N\mathcal{R}}(k_\gamma) = \frac{e}{\sqrt{2\omega_\gamma}}\langle\mathcal{R}|j_{EM}(k_\gamma)|N\rangle,$$

where the resonant state stemming from the second and the third term in (2) consists of the bare-quark part and the meson cloud

$$|\mathcal{R}\rangle = \frac{1}{\sqrt{Z_{\mathcal{R}}}}\left\{|\Phi_{\mathcal{R}}\rangle - \sum_{MB}\int \frac{dk \quad \mathcal{V}^{M}_{B\mathcal{R}}(k)}{\omega_k + E_B - W}\,[a^{\dagger}(k)|\widetilde{\Psi}_B\rangle]^{JT}\right\}. \qquad (14)$$

The background term entering (7) is dominated by the pion-pole term and the u-channel process which originate from the first term in (2).

In Figs. 3 – 6 the transverse photo-production amplitudes for the partial D13, D33 and D15 partial waves calculated in our model are compared to the data as well as to the analysis of the MAID group [11]. While our calculation correctly reproduce the behavior of the amplitudes at the energies close to the threshold where they are dominated by the pion-pole term, their strength in the resonance region is typically a factor 0.5 to 0.7 weaker compared to the value of the electric transverse amplitude as deduced from the experiment, and even weaker in the case of the magnetic amplitude. The pertinent multipoles are sensitive to the

nucleon's periphery which is apparently not adequately reproduced in the bag model, as we have already noticed when analyzing the coupling of the resonance to the d-wave pions. Here the pion cloud effect are relatively weak as a consequence of cancellations of different terms, and contribute at the level of 10 % to 20 % to the amplitudes.

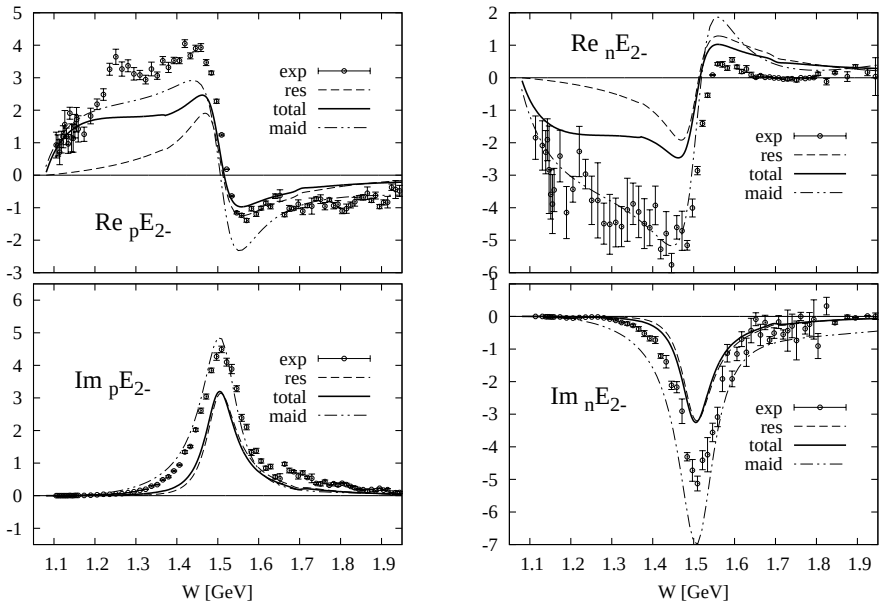

Fig. 3. The real and the imaginary part of the proton and neutron multipoles E_{2-} for the D13 wave in units $10^{-3}/m_\pi$ (preliminary). The data points are from [10], "maid" corresponds to the partial wave analysis from [11].

Nonetheless, we should stress that the amplitudes exhibit a consistent behavior in all considered partial waves. In particular, our model correctly predicts that in the D13 partial wave the ${}_nE_{2-}^{1/2}$ multipole amplitude is weaker than the corresponding ${}_nE_{2-}^{1/2}$ amplitude, and that the ${}_nM_{2-}^{1/2}$ amplitude almost vanishes. Similarly, for the D15 partial wave the quark model predicts that the quark contribution to the ${}_pM_{2-}^{1/2}$ multipole vanishes and only the pion cloud contributes to the resonant part of the amplitude. The non-zero quark contribution in the case of the neutron multipole is however too weak to reproduce the data.

6 Discussion

Comparing the present results with the results for other partial waves obtained in chiral quark models we notice a general trend that the quark core alone does not provide sufficient strength to reproduced the observed resonance excitation amplitudes. The best known example is the P33 partial wave in which case the quark contribution to the electric dipole excitation of the $\Delta(1232)$ is estimated

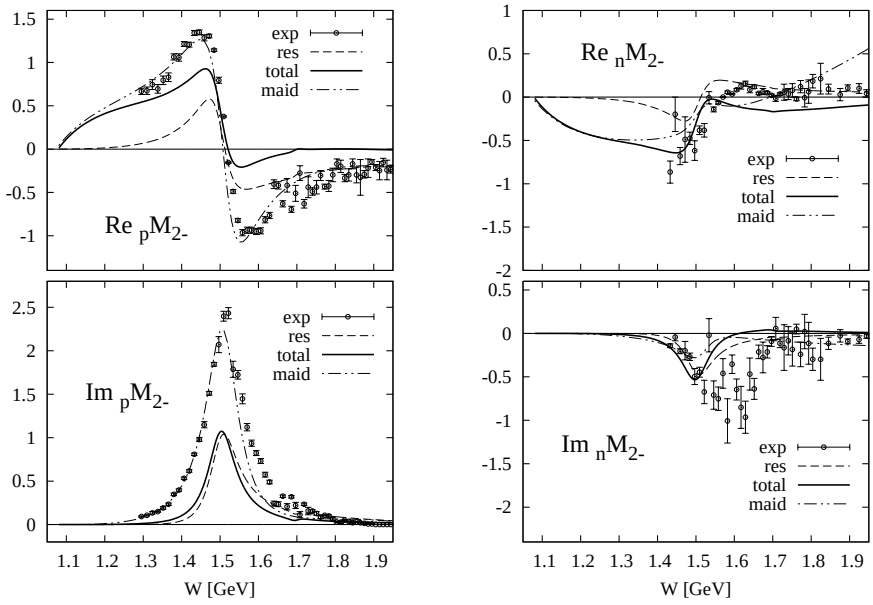

Fig. 4. The M_{2-} multipole, notation as in Fig. 3.

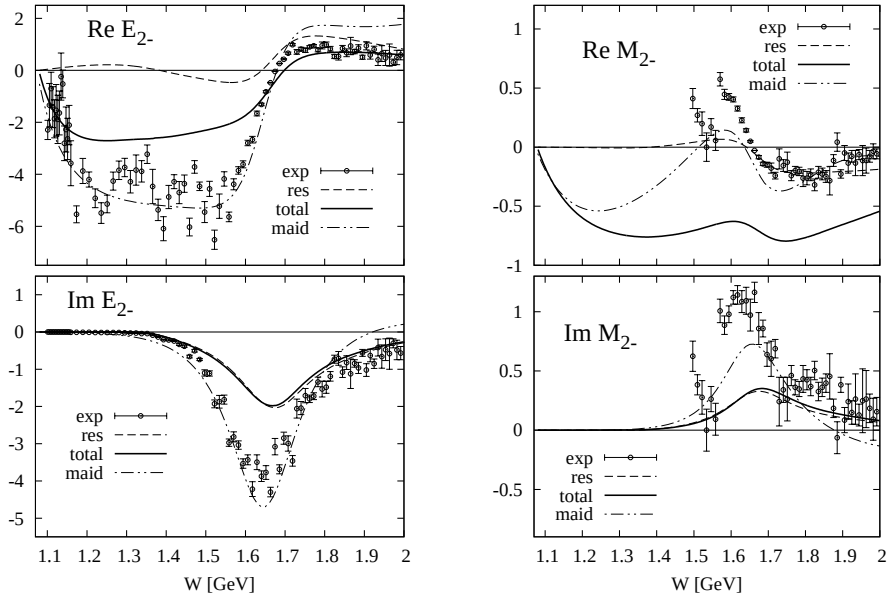

Fig. 5. E_{2-} and M_{2-} amplitudes for the D33 wave, notation as in Fig. 3.

by only 60 % while the rest is attributed to the pion cloud [1]. In the present calculation the pion cloud effects turn out not to be that important. In fact, we have noticed a considerable cancellation of different contributions of the meson cloud, e.g. the vertex correction due to pion loops and the genuine contribution

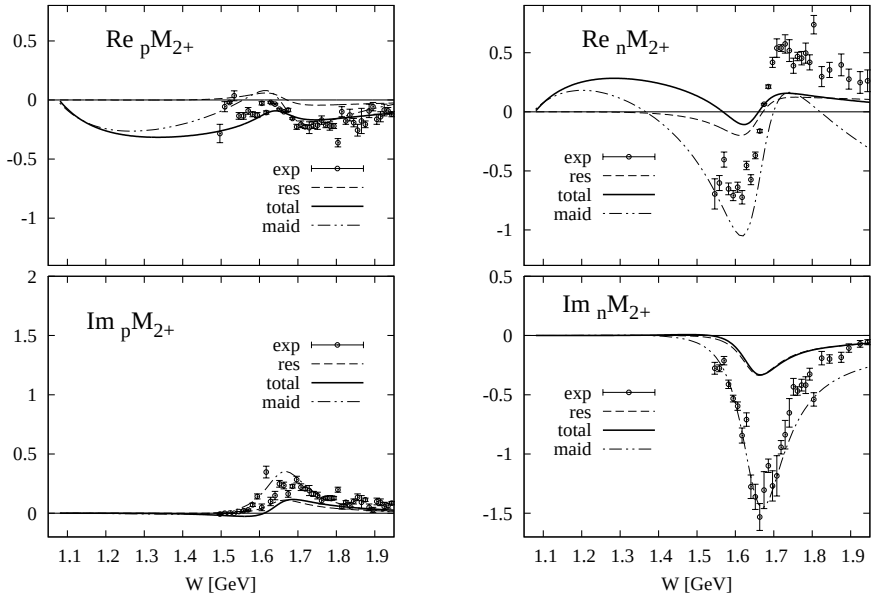

Fig. 6. The M_{2+} amplitudes for the D15 wave, notation as in Fig. 3.

of the pion cloud to the EM current. It is therefore possible that a calculation in a more elaborate chiral quark model could provide a better agreement with the data. To conclude, the overall qualitative agreement with the multipole analysis in the D13, D33 and D15 partial waves prove that the quark-model explanation of the D-wave resonance as the p-wave excitation of the quark core supplemented by the meson cloud is sensible and that no further degrees of freedom are needed.

References

1. M. Fiolhais, B. Golli, S. Širca, Phys. Lett. B **373**, 229 (1996)
2. P. Alberto, M. Fiolhais, B. Golli, and J. Marques, Phys. Lett. B **523**, 273 (2001).
3. B. Golli, S. Sirca, L. Amoreira, M. Fiolhais Phys.Lett. B553 (2003) 51-60
4. P. Alberto, L. Amoreira, M. Fiolhais, B. Golli, and S. Širca, Eur. Phys. J. A **26**, 99 (2005).
5. B. Golli and S. Širca, Eur. Phys. J. A **38**, (2008) 271.
6. B. Golli, S. Širca, and M. Fiolhais, Eur. Phys. J. A **42**, 185 (2009)
7. B. Golli, S. Širca, Eur. Phys. J. A **47** (2011) 61.
8. B. Golli, talk given at the Sixth International Workshop on Pion-Nucleon Partial-Wave Analysis and the Interpretation of Baryon Resonances, 23–27 May, 2011, Washington, DC, U.S.A., `http://gwdac.phys.gwu.edu/pwa2011/Thursday/b_golli.pdf`
9. Simon Širca, Bojan Golli, Manuel Fiolhais and Pedro Alberto, in Proceedings of the XIV International Conference on Hadron Spectroscopy (hadron2011), Munich, 2011, edited by B. Grube, S. Paul, and N. Brambilla, eConf C110613 (2011) [`http://arxiv.org/abs/1109.0163`].
10. R. A. Arndt, W. J. Briscoe, I. I. Strakovsky, R. L. Workman, Phys. Rev. C **74** (2006) 045205.
11. D. Drechsel, S.S. Kamalov, L. Tiator, Eur. Phys. J. A **34**, 69 (2007).

Bled Workshops
in Physics
Vol. 13, No. 1
p. 74

Proceedings of the Mini-Workshop
Hadronic Resonances
Bled, Slovenia, July 1 - 8, 2012

Scattering phase shifts and resonances from lattice QCD

S. Prelovšek[a,b]

[a] Jožef Stefan Institute, Jamova 39, 1000 Ljubljana, Slovenia
[b] Faculty of Mathematics and Physics, University of Ljubljana, Jadranska 19, 1000 Ljubljana, Slovenia

Most of hadrons are hadronic resonances - they decay quickly via the strong interactions. Among all the resonances, only the ρ meson has been properly simulated as a resonance within lattice QCD up to know. This involved the simulation of the ππ scattering in p-wave, extraction of the scattering phase shift and determination of m_R and Γ via the Breit-Wigner like fit of the phase shift.

In the past year, we performed first exploratory simulations of Dπ, D*π and Kπ scattering in the resonant scattering channels [1,2]. Our simulations are done in lattice QCD with two-dynamical light quarks at a mass corresponding to $m_\pi \simeq$ 266 MeV and the lattice spacing $a = 0.124$ fm.

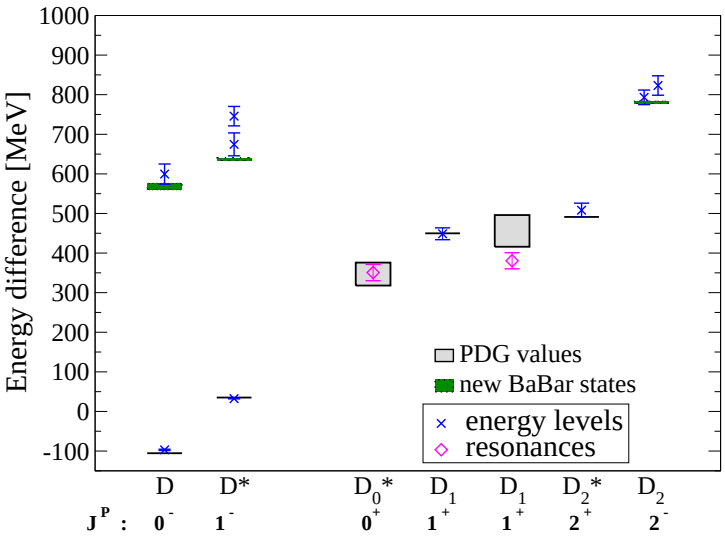

Fig. 1. Energy differences $\Delta E = E - \frac{1}{4}(M_D + 3M_{D^*})$ for D meson states in our simulation [1] and in experiment; the reference spin-averaged mass is $\frac{1}{4}(M_D + 3M_{D^*}) \approx 1971$ MeV in experiment. Magenta diamonds give resonance masses for states treated properly as resonances, while those extracted naively assuming $m_n = E_n$ are displayed as blue crosses [1].

The masses and widths of the broad scalar $D_0^*(2400)$ and the axial $D_1(2430)$ charmed-light resonances are extracted by simulating the corresponding $D\pi$ and $D^*\pi$ scattering on the lattice [1]. The resonance parameters are obtained using a Breit-Wigner fit of the elastic phase shifts. The resulting $D_0^*(2400)$ mass is 351 ± 21 MeV above the spin-average $\frac{1}{4}(m_D + 3m_{D^*})$, in agreement with the experimental value of 347 ± 29 MeV above. The resulting $D_0^* \to D\pi$ coupling $g^{lat} = 2.55 \pm 0.21$ GeV is close to the experimental value $g^{exp} = 1.92 \pm 0.14$ GeV, where g parametrizes the width $\Gamma \equiv g^2 p^\star/s$. The resonance parameters for the broad $D_1(2430)$ are also found close to the experimental values; these are obtained by appealing to the heavy quark limit, where the neighboring resonance $D_1(2420)$ is narrow. The simulation of the scattering in these channels incorporates quark-antiquark as well as $D^{(*)}\pi$ interpolators, and we use distillation method for contractions. The resulting D-meson spectrum is compared to the experimental one in Fig. 1.

In addition, the ground and several excited charm-light and charmonium states with various J^P are calculated using standard quark-antiquark interpolators. The lattice results for the charmonium are compared to the experimental levels in Fig. 2.

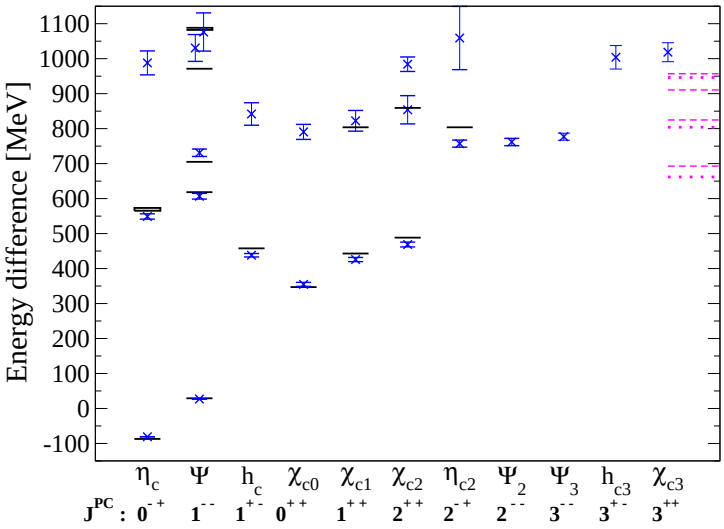

Fig. 2. Energy differences $\Delta E = E - \frac{1}{4}(M_{\eta_c} + 3M_{J\psi})$ for charmonium states in our simulation [1] and in experiment; reference spin-averaged mass is $\frac{1}{4}(M_{\eta_c} + 3M_{J\psi}) \approx 3068$ MeV in experiment. The magenta lines on the right denote relevant lattice and continuum $\bar{D}^{(*)}D^{(*)}$ thresholds.

We also simulated $K\pi$ scattering in s-wave and p-wave for both isospins $I = 1/2,\ 3/2$ using quark-antiquark and meson-meson interpolating fields [2]. Fig. 3 shows the resulting energy levels of $K\pi$ in a box. In all four channels we observe the expected $K(n)\pi(-n)$ scattering states, which are shifted due to the interaction. In both attractive $I = 1/2$ channels we observe additional states that are related

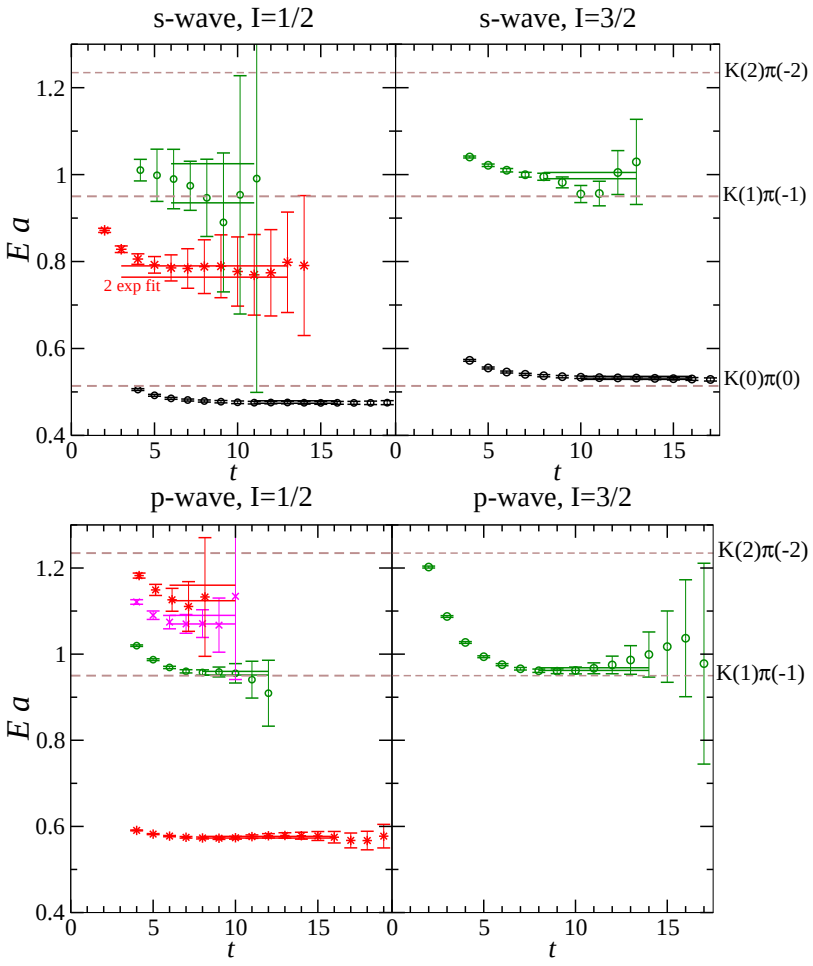

Fig. 3. The energy levels $E(t)a$ of the $K\pi$ in the box for all four channels (multiply by $a^{-1} = 1.59$ GeV to get the result in GeV). The horizontal broken lines show the energies $E = E_K + E_\pi$ of the non-interacting scattering states $K(n)\pi(-n)$ as measured on our lattice; $K(n)\pi(-n)$ corresponds to the scattering state with $p^* = \sqrt{n}\frac{2\pi}{L}$. Note that there is no $K(0)\pi(0)$ scattering state for p-wave. Black and green circles correspond to the shifted scattering states, while the red stars and pink crosses correspond to additional states related with resonances.

to resonances; we attribute them to $K_0^*(1430)$ in s-wave and $K^*(892)$, $K^*(1410)$ and $K^*(1680)$ in p-wave. We extract the elastic phase shifts δ at several values of the $K\pi$ relative momenta. The resulting phases exhibit qualitative agreement with the experimental phases in all four channels, as shown in Fig. 4. In addition to the values of the phase shifts shown in Fig. 4, we also extract the values of the phase shift close to the threshold, which are expressed in terms of the scattering lengths in [2].

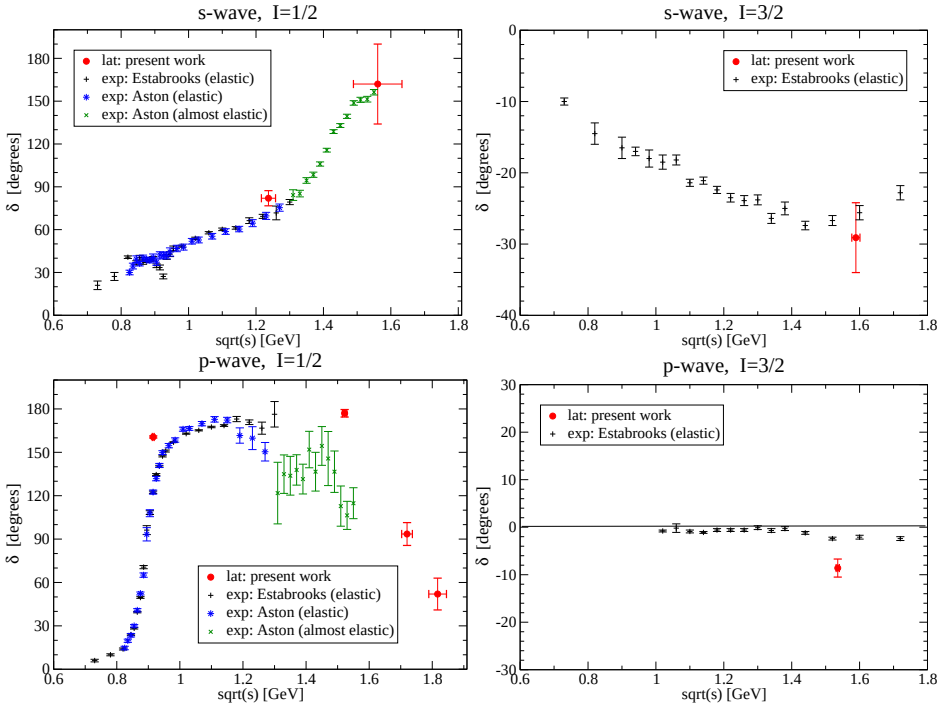

Fig. 4. The extracted $K\pi$ scattering phase shifts δ_ℓ^I in all four channels $l = 0, 1$ and $I = 1/2,\ 3/2$. The phase shifts are shown as a function of the $K\pi$ invariant mass $\sqrt{s} = M_{K\pi} = \sqrt{(p_\pi + p_K)^2}$. Our results (red circles) apply for $m_\pi \simeq 266$ MeV and $m_K \simeq 552$ MeV in our lattice simulation. In addition to the phases provided in four plots, we also extract the values of $\delta_0^{1/2,\ 3/2}$ near threshold $\sqrt{s} = m_\pi + m_K$, but these are provided in the form of the scattering length in the main text (as they are particularly sensitive to $m_{\pi,K}$). Our lattice results are compared to the experimental elastic phase shifts (both are determined up to multiples of 180 degrees).

We believe that these simulations of the $D\pi$, $D^*\pi$ and $K\pi$ scattering in the resonant channels represent encouraging step to simulate resonances properly from first principle QCD. There are many other exciting resonances waiting to be simulated along the similar lines.

References

1. D. Mohler, S. Prelovsek and R. Woloshyn, $D\pi$ *scattering and* D *meson resonances from lattice QCD*, `arXiv:1208.4059`.
2. C. B. Lang, Luka Leskovec, Daniel Mohler, Sasa Prelovsek, $K\pi$ *scattering for isospin 1/2 and 3/2 in lattice QCD*, Phys. Rev. D.86. (2012) 054508, `arXiv:1207.3204`.